Journal of Power Sources 187 (2009) 190–203

Contents lists available at ScienceDirect

Journal of Power Sources

journal homepage: www.elsevier.com/locate/jpowsour

Design of a thermally integrated bioethanol-fueled solid oxide fuel cell system integrated with a distillation column

W. Jamsak[a], P.L. Douglas[b,*], E. Croiset[b], R. Suwanwarangkul[c], N. Laosiripojana[d], S. Charojrochkul[e], S. Assabumrungrat[a]

[a] Center of Excellence in Catalysis and Catalytic Reaction Engineering, Department of Chemical Engineering, Faculty of Engineering, Chulalongkorn University, Thailand
[b] Department of Chemical Engineering, University of Waterloo, Canada
[c] School of Bio-Chemical Engineering and Technology, Sirindhorn International Institute of Technology, Thammasart University-Rangsit Campus, Patum Thani 12121, Thailand
[d] The Joint Graduate School of Energy and Environment, King Mongkut's University of Technology, Thonburi, Thailand
[e] National Metal and Materials Technology Center (MTEC), Thailand

ARTICLE INFO

Article history:
Received 21 May 2008
Received in revised form 1 September 2008
Accepted 2 September 2008
Available online 20 September 2008

Keywords:
Solid oxide fuel cell
Integration
Bioethanol
Distillation unit
Heat exchanger network

ABSTRACT

Solid oxide fuel cell systems integrated with a distillation column (SOFC-DIS) have been investigated in this study. The MER (maximum energy recovery) network for SOFC-DIS system under the base conditions (C_{EtOH} = 25%, EtOH recovery = 80%, V = 0.7 V, fuel utilization = 80%, T_{SOFC} = 1200 K) yields Q_{Cmin} = 73.4 and Q_{Hmin} = 0 kW. To enhance the performance of SOFC-DIS, utilization of internal useful heat sources from within the system (e.g. condenser duty and hot water from the bottom of the distillation column) and a cathode recirculation have been considered in this study. The utilization of condenser duty for preheating the incoming bioethanol and cathode recirculation for SOFC-DIS system were chosen and implemented to the SOFC-DIS (CondBio-CathRec). Different MER designs were investigated. The obtained MER network of CondBio-CathRec configuration shows the lower minimum cold utility (Q_{Cmin}) of 55.9 kW and total cost index than that of the base case. A heat exchanger loop and utility path were also investigated. It was found that eliminate the high temperature distillate heat exchanger can lower the total cost index. The recommended network is that the hot effluent gas is heat exchanged with the anode heat exchanger, the external reformer, the air heat exchanger, the distillate heat exchanger and the reboiler, respectively. The corresponding performances of this design are 40.8%, 54.3%, 0.221 W cm^{-2} for overall electrical efficiency, Combine Heat and Power (CHP) efficiency and power density, respectively. The effect of operating conditions on composite curves on the design of heat exchanger network was investigated. The obtained composite curves can be divided into two groups: the threshold case and the pinch case. It was found that the pinch case which T_{SOFC} = 1173 K yields higher total cost index than the CondBio-CathRec at the base conditions. It was also found that the pinch case can become a threshold case by adjusting split fraction or operating at lower fuel utilization. The total cost index of the threshold cases is lower than that of the pinch case. Moreover, it was found that some conditions can give lower total cost index than that of the CondBio-CathRec at the base conditions.

1. Introduction

A Solid Oxide Fuel Cell (SOFC) is known as one of potential power generator because of its high systematic efficiency, wide range of applications, and fuel flexibility. Typically, due to the high operating temperature of SOFC and the remain of unreacted fuels from the SOFC stack, the high temperature effluent and the combustion heat of unreacted fuels can be thermally utilized to other parts of the system. In general, there are two possible options to utilize high temperature effluent and enhance high SOFC system performance, i.e. Solid Oxide Fuel Cell with Gas Turbine system (SOFC-GT) and Solid Oxide Fuel Cell with Combined Heat and Power system (SOFC-CHP). It should be noted that SOFC-CHP is the main focus in the present work.

Typically, SOFC-CHP system consists of preheaters, an SOFC stack and an afterburner. A reformer is also required when other compounds apart from hydrogen were used as the primary feed. According to the operation, the unreacted fuels and excess air from the stack are burnt in the afterburner to generate more heat. Until now, several configurations of the SOFC system have been proposed. Fontell et al. [1] and Zhang et al. [3] studied natural gas-fed system integrated with a desulfurization unit. According

* Corresponding author. Tel.: +1 519 888 4601; fax: +1 519 888 4365.
E-mail address: pdouglas@uwaterloo.ca (P.L. Douglas).

0378-7753/$ – see front matter © 2008 Elsevier B.V. All rights reserved.
doi:10.1016/j.jpowsour.2008.09.036

Nomenclature

C_{EtOH}	ethanol concentration [mol%]
E	electromotive force of a cell [V]
E_a	activation energy [J mol^{-1}]
F	Faraday constant [C mol^{-1}]
i	current density [A cm^{-2}]
I	current [A]
LHV_{EtOH}	lower heating value of ethanol [J mol^{-1}]
n_{EtOH}	total ethanol flow rate fed to the distillation column [mol s^{-1}]
p_i	partial pressure of component i [kPa]
P	pressure [kPa]
P_{den}	power density [A cm^{-2}]
Q_1	energy required for Preheater 1 [kW]
Q_2	energy required for Preheater 2 [kW]
Q_3	energy required for a reformer [kW]
Q_4	energy required for Preheater 4 [kW]
Q_5	energy left in a bottom stream of the distillation column [kW]
Q_6	energy involved with the combustion of exhausted gases after being cooled to the exit temperature [kW]
Q_{Con}	condenser duty [kW]
Q_{Net}	net useful heat [kW]
Q_{Reb}	reboiler duty [kW]
$Q_{SOFC,Net}$	net exothermic from SOFC [kW]
r	area specific resistance [Ω cm^2]
r_{act}	activation polarization area specific resistance [Ω cm^2]
r_{ohm}	ohmic polarization area specific resistance [Ω cm^2]
$r_{H_2,cons}$	rate of hydrogen consumed by the electrochemical reaction [mol s^{-1}]
R	gas constant [J mol^{-1} K^{-1}]
Sp	split faction
$T_{anode,in}$	anode inlet temperature [K]
$T_{cath,in}$	cathode inlet temperature [K]
T_{RF}	reforming temperature [K]
T_{SOFC}	SOFC temperature [K]
U_f	fuel utilization [%]
V	operating voltage [V]
W_e	electrical power [kW]

Greek letters

η_{CHP}	CHP efficiency [%]
$\eta_{elec,ov}$	overall electrical efficiency [%]
ρ	resistivity [Ω cm]

Subscripts

a	anode
c	cathode

to the configuration in Fontell's work, the anode effluent provided heat to the anode incoming stream and was then split into two streams; the first stream was burnt with the air effluent from the cathode in the afterburner, whereas the second one was recirculated and mixed with the inlet stream before being fed to the pre-reformer. The exhaust gas from the afterburner preheated both water stream and the sulfur-free stream. Regarding Zhang's work, the split of anode outlet stream was also applied but it was not used for preheating the incoming anode stream; the exhaust gas from the afterburner was only used to heat the air inlet stream and the pre-reformer was operated under adiabatic condition. Omosun et al. [2] studied biomass-fueled SOFC system and compared between hot and cold processes. According to the cold process, the anode and cathode effluent preheated the incoming anode and cathode stream, respectively, before being burnt in the afterburner. On the contrary, there is no use of anode effluent to heat the incoming anode stream for the hot process. They reported that the heat management of hot process gave the superior electrical and overall efficiency to that of the cold process; however, the cost of the hot process is higher than that of the cold process due to the fluidized bed gasifier and the hot ceramic filter. Braun et al. [4] studied an anode supported SOFC with micro CHP for residential applications. The effect of fuel types (hydrogen/methane), mode of methane reforming (internal/external reforming), fuel processing with anode recirculation, oxidant processing with cathode recirculation and the combination of recycle and internal reforming on the system performance were investigated. The results showed that the methane-fueled system with cathode and anode recirculation with internal reforming yielded the highest efficiency among all designs. System electrical efficiency and CHP efficiency are 40% (HHV) and 79% (HHV), respectively.

A few investigations on ethanol-fed SOFC system have previously been published. Generally, ethanol-fed SOFC system consists of a vaporizer, preheaters, a reformer, an SOFC stack and an afterburner. Douvartzides et al. [5] used exergy analysis and optimization strategy to investigate the system performance and reported that the exergy loss of SOFC can be minimized by matching the appropriate reforming temperature and air preheating temperature. With the same system configuration, Douvartzides et al. [6] also compared the performance of SOFC system fed by methane with that fueled by ethanol. The exergy analysis indicated that the efficiency of the methane-fed system is higher than that of the ethanol-fed one. Arteaga et al. [7] studied ethanol-fed SOFC system consisting of a mixer, a vaporizer, an ethanol/water mixture heater, a compressor, a reformer, a fuel cell stack and a furnace by using pseudo-homogenous model. They reported that the heating consumption for vaporizing the H_2O/EtOH mixture increases with increasing the steam to EtOH ratio (H_2O:EtOH) and H_2 production initially increases but decreases when the H_2O:EtOH ratio is higher than 8. In addition, the increase of reforming temperature promoted the fuel cell efficiency and decreases energy required for heating up the synthesis gas before reaching SOFC stack; however, the higher energy consumption for the external reformer is also required.

Most of the previous studies on the ethanol-fed SOFC system have been carried out by using pure ethanol mixed with water. From an energy point of view, it is not efficient and necessary to purify bioethanol to highly pure ethanol as some water is usually required for the steam reforming reaction. Therefore, purifying bioethanol just to reach a desired ethanol concentration needed for the steam reforming is adequate. The SOFC system implemented with a distillation column (SOFC-DIS) has been considered in our previous work [8]. The hot effluent from the afterburner was used for heating all heaters, an external reformer and a boiler of a distillation column. The possibility to operate the SOFC-DIS as a self energy-sufficient system was examined. It was found that the SOFC-DIS system can operate without an external heat source. Nevertheless, the calculation in our previous study was based on the direct subtraction between net supply energy and net consumption energy in the system, and no details on heat transfer arrangement were considered. Moreover, other useful heat in the system (e.g. condenser duty and hot water at the bottom of the distillation column) were not utilized. Also, the high temperature of air coming out from the cathode should also be considered as the SOFC stack is usually operated under excess air.

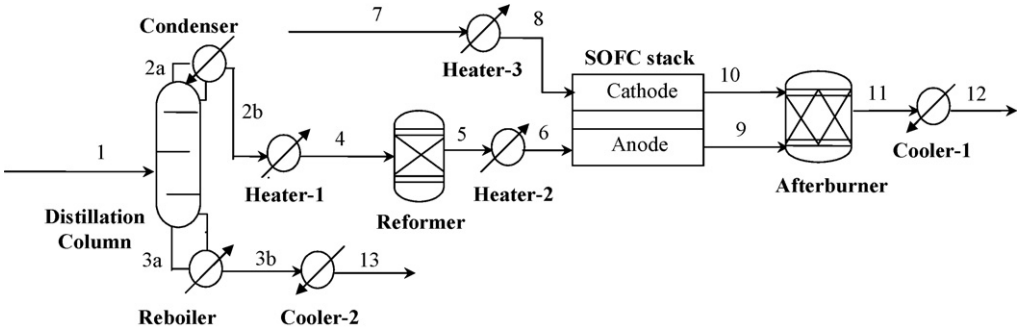

Fig. 1. Schematic diagram of base case SOFC-DIS systems at the base conditions (C_{EtOH} = 25%, EtOH recovery = 80%, U_f = 80%, V = 0.7 V, T_{SOFC} = 1200 K, $T_{anode,in}$ = 1100 K, $T_{cath,in}$ = 1000 K, T_{RF} = 1023 K and P = 101.3 kPa).

The main objective of this work is to study the performance of the SOFC-DIS when all heat transfer is considered. Moreover, other useful heat, e.g. condenser duty and hot water from the bottom of the column and the cathode recirculation are taking into account to enhance the performance of SOFC-DIS. In addition, the effect of operating conditions on composite curve is also examined and lastly the designs of the heat exchanger network for the SOFC-DIS system are further investigated.

2. SOFC-DIS process system modelling using Aspen Plus™

Fig. 1 shows the simplified process flow diagram of the SOFC-DIS system; the SOFC-DIS system was simulated using Aspen Plus™ 2006.

The SOFC-DIS system consists of a distillation column, an external reformer, heaters, coolers, an SOFC stack and an afterburner. Bioethanol containing 5 mol% ethanol (C_2H_5OH) is introduced to the distillation column at atmospheric pressure and 298 K and purified to a desired concentration. Thereafter, the concentrated ethanol is fed to the Heater-1 prior to entering the external reformer in order to reform ethanol to H_2. The synthesis gas from an external reformer is further heated by Heater-2 and fed to an anode side of the SOFC stack for producing electricity. The air stream is heated in Heater-3 and then fed to the cathode side of the SOFC stack. The exhaust gas from the SOFC stack containing small amount of unused fuel enters the afterburner where excess fuel is combusted to produce additional heat for use in the system. The heat recovery from the post-combustion stream can be calculated by cooling the hot effluent from the afterburner to 403 K before emitting to the surrounding.

The *Peng–Robinson* thermodynamic option set, suitable for non-polar light components, was used for all units except the distillation column; the *UNIFAC* activity coefficient model was used in the distillation column.

One design-spec was used in simulation. *Design-spec*-1 was used to adjust incoming bioethanol flow rate (stream 1) to reach the fuel utilization target. In addition, the stack area also keeps constant by using calculated current density and the operation of *Design-spec-1*. The target fuel utilization and voltage was set. The calculations of mass balance, energy balance and performances were performed inside the user-subroutine SOFC. The calculated mass, enthalpy and other physical properties (i.e. density, molecular weight) of anode and cathode stream were sent through material stream numbers 9 and 10, respectively. The details of modelling for each unit in the system are described below.

2.1. Distillation column

The distillation column is modelled using Aspen Plus™ rigorous distillation model, *RadFrac*. A partial condenser and a kettle reboiler are used in this study. Four stages are sufficient to purify bioethanol until it reaches the concentration of 41 mol% with 99% recovery. It should be noted that 41 mol% is the maximum ethanol concentration that can be fed to the external reformer without carbon formation [9]. *UNIFAC* which is suitable for polar systems, in this case the mixture of ethanol and water, at atmospheric pressure is used as a thermodynamics equation for the distillation column. A *RadFrac* built-in *Design-spec* was used to adjust the distillate rate and reflux ratio to obtain the desired ethanol concentration and recovery.

2.2. Ethanol reformer

In this study, an *RGibbs* reactor model was used for simulating the external reformer. Previous experimental results confirmed that a gas mixture at thermodynamic equilibrium contains only five components with noticeable concentration: i.e. carbon monoxide, carbon dioxide, hydrogen, steam, and methane [10,11]. Therefore, these five components and one more ethanol component are modelled in the reactor.

2.3. SOFC stack

The SOFC stack is simulated by using a user-subroutine named *USRUSR*. The subroutine contains mass and energy balance equations and SOFC performance equations. For the mass balance, the synthesis gas which contains CO, CO_2, H_2, CH_4 and H_2O is fed to the SOFC stack. Only water gas shift reaction and electrochemical reactions take place inside the SOFC stack as shown in the following equations.

$$CO + H_2O = H_2 + CO_2 \quad (1)$$

$$H_2 + \tfrac{1}{2}O_2 \rightarrow H_2O \quad (2)$$

It should be bear in mind that water gas shift reaction is fast equilibrium reaction. Ethanol reforming is not considered in the stack as trace amount of ethanol is present in the product stream for the reformer. In addition, methanation hardly takes place at high temperature. Therefore, both reactions can be neglected in calculations. The components inside the SOFC stack were calculated based on thermodynamics calculation. The performance of the SOFC was calculated by equilibrium components inside the stack and based on one-dimensional calculation. Details of SOFC model including

Table 1
Parameters for activation loss [12].

r_{act} ($\Omega\,cm^2$)	k ($\times 10^{-13}$ A cm^2)	E_a (kJ mol^{-1} K^{-1})	m
$r_{act,c}$	14.9	160	0.25
$r_{act,a}$	0.213	110	0.25

Table 2
Parameters of ohmic loss in SOFC cell components [13].

Materials	Parameters		Thickness (μm)
	α (Ω cm)	β (K)	
Anode (40% Ni/YSZ cermet)	2.98×10^{-5}	−1392	150
Cathode (Sr-doped $LaMnO_3$:LSM)	8.11×10^{-5}	600	2000
Electrolyte (Y_2O_3-doped ZrO_2:YSZ)	2094×10^{-5}	10350	40
Interconnect (Mg-doped $LaCrO_3$)	1.256×10^{-3}	4690	100

performance calculations are presented in Tables 1 and 2 and in our previous work [8]. The energy balance equation, the SOFC stack operates under steady state and adiabatic condition. The energy equation can be calculated by enthalpy change and power around the SOFC stack as presented in Eq. (3).

$$0 = H_{fuel,in} + H_{air,in} - H_{fuel,out} - H_{air,out} - W_e \quad (3)$$

Because the inlet and outlet temperature of the streams was set, the required amount of air was then calculated.

2.4. Afterburner

The afterburner was modelled using the *Rstoic*, stoichiometric reactor model. All unreacted products from an SOFC stack (e.g. CH_4, CO, and H_2) are reacted with the unreacted O_2 as shown in Eqs. (4)–(6). The complete combustion is assumed. It should be noted that ethanol is not present in the afterburner due to complete ethanol reforming [8]. In this study, N_2 is assumed to be inert and no NO_X is produced.

$$CH_4 + 2O_2 \rightarrow CO_2 + 2H_2O \quad (4)$$

$$CO + \tfrac{1}{2}O_2 \rightarrow CO_2 \quad (5)$$

$$H_2 + \tfrac{1}{2}O_2 \rightarrow H_2O \quad (6)$$

2.5. Heaters and coolers

Heaters and coolers were modelled using the *Heater* model in Aspen Plus™. One only needs to supply the desired exit temperature and the model calculates the heat duty resulting from the change in enthalpy between the inlet and the specified outlet.

2.6. Performance definition

In this study, overall electrical efficiency and CHP efficiency can be calculated as

$$\eta_{elec,ov} = \frac{W_e}{(n_{EtOH} \times LHV_{EtOH}) + Q_{ext}} \quad (7)$$

$$\eta_{CHP} = \frac{W_e + Q_U}{(n_{EtOH} \times LHV_{EtOH}) + Q_{ext}} \quad (8)$$

where W_e represents the electrical power, LHV_{EtOH} the low heating value of ethanol, $\eta_{elec,ov}$ the overall electrical efficiency, η_{CHP} the Combine Heat and Power (CHP) efficiency, Q_U the net heat produced by the SOFC-DIS system after heat exchanging with heaters and a reboiler, Q_{ext} the external heat from an external heat source, Q_k the energy consumption at Heater k, Q_{Reb} the reboiler duty.

2.7. Heat exchanger network

The obtained information from Aspen Plus™ was used to design heat exchanger network by using Aspen Plus™ HX-NET module (version 2006). The input data for HX-Net is initial temperature, temperature target and enthalpy change. The effect of operating conditions (i.e. ethanol concentration, ethanol recovery, fuel utilization, voltage and split fraction) on the composite curves and the design of heat exchanger network was also investigated. Hot utility and cold utility used in this work are fired heat and cooling water, respectively. For costing, five year was used for the operating period.

2.8. System configuration study

In this work, condenser duty, hot water from the bottom of the column and cathode recirculation were also considered to enhance the performance of SOFC-DIS. Since hot water at the bottom and condenser duty is low-temperature heat source, the application of these types of heat is to preheat incoming low-temperature reactants, in this case, incoming air or bioethanol. Four additional configurations are listed as below.

- Case a: No thermal heat integration (No-HX).
- Case b: Utilization of heat from the condenser to incoming bioethanol (CondBio).
- Case c: Utilization of heat from hot water at the bottom of the column to incoming bioethanol (HW-Cond).
- Case d: Utilization of heat from the condenser to incoming air (Cond-Air).
- Case e: Implementation of cathode recirculation (CathRec).

All options were compared and a suitable configuration was chosen for further design of heat exchanger network of SOFC-DIS. The discussion will be presented in the following section.

3. Results and discussion

3.1. Heat exchanger network for base case SOFC-DIS

The base case of the SOFC-DIS is illustrated by Fig. 1. All cold process streams, which need to be heated, were heated using a hot utility to reach the target temperatures. Likewise, all hot process streams, which need to be cooled, were cooled using a cold utility. The minimum temperature difference for heat exchange was fixed at 10 K and it was assumed that the heat capacity of all streams was constant during heat exchanging process. Cooling water at 293.2 K and fired heat at 1273.2 K were selected as cold and hot utilities

Table 3
Operating parameters at base conditions.

Parameter	Value/quality
Fuel option	Bioethanol with 5 mol%
C_{EtOH}	25 mol%
Ethanol recovery	80%
U_f	80%
Voltage	0.7 V
T_{SOFC}	1200 K
T_{RF}	1023 K
$T_{anode,in}$	1100 K
$T_{cath,in}$	1000 K
P	101.3 kPa

Table 4
Information of hot and cold streams at the base case SOFC-DIS (No-HX).

Stream no.	Stream label	T_{in} (K)	T_{out} (K)	Load (kW)	MC_p (kW K^{-1})
Hot stream					
Cooler-1 (11–12)	H1	1304.9	403.0	847.3	0.940
Condenser (2a–2b)	H2	365.9	365.9	48.8	Large
Cooler-2 (3b–13)	H3	369.3	303.2	45.4	0.687
Cold stream					
Air stream (7b–8)	C1	298.2	1000.0	580.7	0.827
BioEtOH stream (1)	C2	298.2	–	–	–
Anode heater (5–6)	C3	1023.0	1100.0	7.3	0.095
Distillate stream (2–4)	C4	365.9	1023.0	50.9	0.078
Reboiler (3a–3b)	C5	298.2	369.3	149.1	2.097
Reformer (4–5)	C6	1023.0	1023.0	85.4	Large

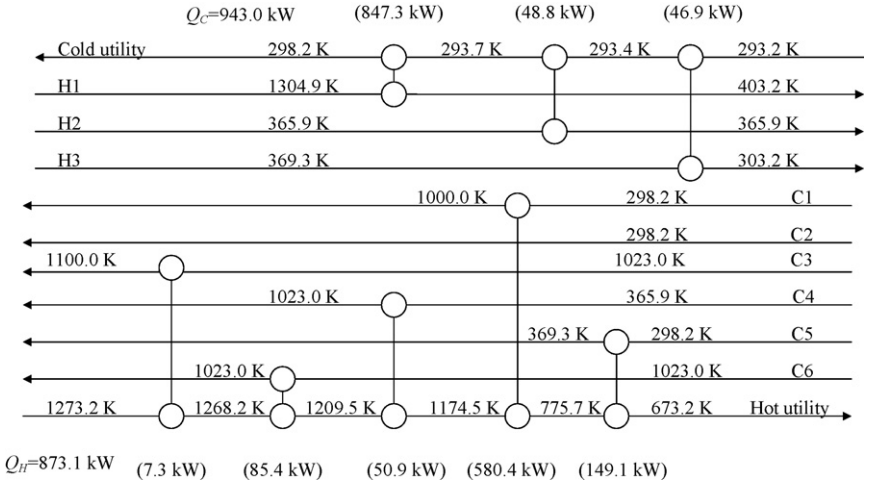

Fig. 2. Heat exchanger network of base case SOFC-DIS (No-HX) at the base conditions (C_{EtOH} = 25%, EtOH recovery = 80%, U_f = 80%, V = 0.7 V, T_{SOFC} = 1200 K, $T_{anode,in}$ = 1100 K, $T_{cath,in}$ = 1000 K, T_{RF} = 1023 K and P = 101.3 kPa).

respectively. The base operating conditions, shown in Table 3, are C_{EtOH} = 25 mol%, EtOH recovery = 80%, V = 0.7 V, U_f = 80%, T_{RF} = 1023 K and T_{SOFC} = 1200 K. The starting temperature, target temperature, heat load and heat capacity of all hot and cold streams for the base case are presented in Table 4. The heat exchanger network involving only utility heaters and coolers for the base case is presented in Fig. 2. It can be seen that the major energy consumers are *Heater-2*, the air preheater (580.4 kW or 66.5% of the overall energy consumption) and the reboiler (149.1 kW or 17.1% of the overall energy consumption); the net energy consumption is 873.1 kW which is supplied by the hot utility. It can be seen that the hot stream from the afterburner is the major energy supplier and contains 847.3 kW of thermal energy which, in this case, corresponds to the cooling energy by the cold utility. Electrical power of 220.5 kW is produced. The overall electrical efficiency, CHP efficiency and corresponding power density of SOFC-DIS are 15.8%, 76.5% and 0.229 W cm^{-2}, respectively.

The composite curves at the base conditions, when the minimum temperature difference (ΔT_{min}) is set at 10 K, are shown in Fig. 3. The cold composite curve move closely until it reaches ΔT_{min} so as to yield the maximum energy recovery. As shown in Fig. 3, the composite curves become the threshold case where no pinch point occurred; in other words, the composite curves were adjusted to reduce the hot and cold utilities and the need for a hot utility was eliminated before the curves pinched. From the composite curve results, the minimum heating utility required is Q_{Hmin} = 0 and the minimum cooling utility required is Q_{Cmin} = 73.4 kW. In practical terms, this means that we can eliminate entirely the need for a hot utility of 873.1 kW shown in Fig. 2, by appropriate heat exchange; we will, however, still need to buy a small amount of cooling utility. The next step is to design an appropriate MER (maximum energy recovery) network, i.e. one that results in $Q_H = Q_{Hmin}$ and $Q_C = Q_{Cmin}$. Note that it is impossible to find a network that will result in $Q_H < Q_{Hmin}$ or $Q_C < Q_{Cmin}$ at the current design and operating conditions. An example of MER network of the base conditions is shown in Fig. 4. Obviously, the utility can be reduced to $Q_c = Q_{Hmin} = 0$ and $Q_c = Q_{Cmin}$ = 73.4 kW. It can be seen that the hot effluent gas after the afterburner (stream no. 11) is heat exchanged with the anode inlet stream (C3) first and then the reformer (C6), the distillate stream (C4), the air stream (C1) and finally the reboiler

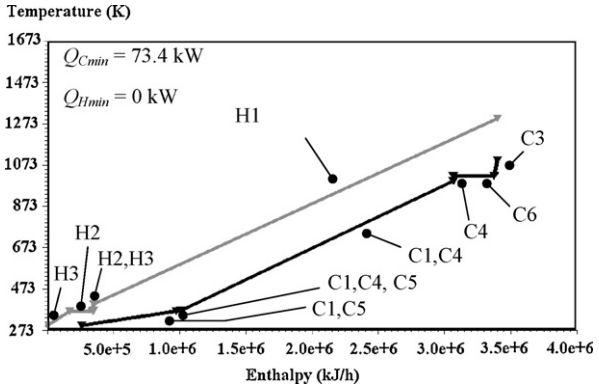

Fig. 3. Composite curves of SOFC-DIS at base conditions (C_{EtOH} = 25%, EtOH recovery = 80%, U_f = 80%, V = 0.7 V, T_{SOFC} = 1200 K, $T_{anode,in}$ = 1100 K, $T_{cath,in}$ = 1000 K, T_{RF} = 1023 K and P = 101.3 kPa).

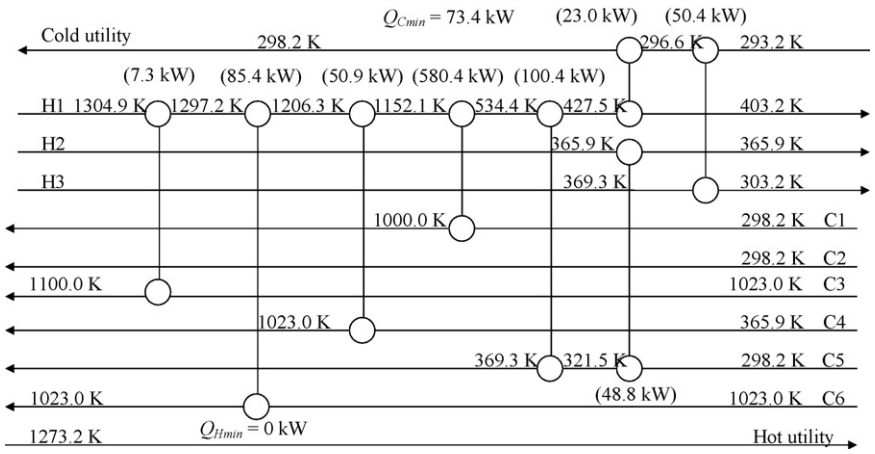

Fig. 4. MER network of SOFC-DIS at the base conditions (C_{EtOH} = 25%, EtOH recovery = 80%, U_f = 80%, V = 0.7 V, T_{SOFC} = 1200 K, $T_{anode,in}$ = 1100 K, $T_{cath,in}$ = 1000 K, T_{RF} = 1023 K and P = 101.3 kPa).

(C5). However, the hot effluent gases cannot supply heat sufficiently to the reboiler. Some heat from the condenser need to supply heat to the reboiler before the reboiler is heated by the hot effluent gases. This is because if the reboiler is heat exchanged with the effluent gases and afterwards by other hot streams (i.e. the heat from the condenser and the hot water of the bottom of the column), the temperature of the reboiler after heat exchanged with the hot effluent gases will be higher than the starting temperature of the other hot streams. Therefore, the heat cannot be transferred and the hot utility is required. The MER network cannot be obtained. However, it should be noted that providing heat to the reboiler requires two hot streams and causes in the high complexity in operation.

3.2. Effect of process structure and operating conditions

3.2.1. Utilizing internal heat and adjusting process flowsheet

To lower the requirement of cold utility for No-HX case used for cooling down the other hot streams, the useful heat from the overhead vapour stream going to the condenser and the useful heat from hot water from the bottom of the distillation column are used for providing heat to other parts of the system. As mentioned earlier, the heat from the vapour stream going to the condenser and from hot water are low-temperature heat streams. To utilize this heat, preheating incoming reactants (air or bioethanol) is reasonable. Moreover, a large amount of air is introduced to the system in order to cool down the SOFC stack. However, the amount of air is more than that needed for burning unreacted fuels from the anode. Therefore, it appears that some benefits could be gained from thermal integration of the heat from the hot streams (that need to be cooled) to the cool streams (that need to be heated). An investigation of the performance of SOFC-DIS when the cathode recirculation is implemented into the system will be performed. Four different configurations of the system are shown in Fig. 5 with different lines. In this study, the utilization of the heat recovery from the condenser for preheating incoming bioethanol (CondBio) representing by dashed line, the heat recovery from condenser for preheating incoming air (Cond-Air) representing by dotted line, the heat recovery from the hot water from the distillation column for preheating bioethanol (HW-Bio) represented by dash dot line and the implementation of cathode recirculation (CathRec) represented by long dash line are considered. It should be noted that the heat from the vapour stream going to the condenser and from hot water are low-temperature heat streams which are suitable for preheating incoming reactants (air or bioethanol). Moreover, a large amount of cooling air introduced to the SOFC in order to cool down the stack is more than that needed for burning unreacted fuels from the anode. Therefore, some air outlet from the SOFC stack should be split and recycled in the system. Heat exchanger networks of different configurations are presented in Figs. 6–10. The performances (e.g. overall electrical efficiency, CHP efficiency and total cost index) of all configurations have been summarized in Table 5. It should be noted that the total cost index is calculated from the total cost of each configuration divided by the total cost of the base case in which no heat integration is considered. In addition, the total cost is a summation of operating cost from hot utility and cold utility and capital cost of heat exchangers, heaters and a cooler in the system.

Since the bioethanol feed stream is available to the system at 298 K it is sub-cooled and needs heating either in the column (increasing the reboiler heat duty) or prior to entering column via heat exchange with a process stream (reducing the energy consumption in the reboiler). Two options, CondBio and HW-Bio are considered to be logical choices for preheating the bioethanol feed stream. From Table 5, the results show that the CondBio yields a slightly higher CHP efficiency and lower total cost index than does the HW-Bio case. Hot water from the bottom of the distillation column yields 46.9 kW for preheating incoming bioethanol in the HW-Bio case. The heat recovery from the condenser (48.8 kW) is fully utilized for preheating bioethanol because the temperature at the condenser remains constant during heat exchange as shown in Fig. 6. On the other hand, the temperature of the hot water drops while exchanging heat as presented in Fig. 7. Due to higher overall electrical efficiency, high CHP efficiency and lower total cost index, the CondBio configuration is selected for preheating bioethanol.

To preheat the incoming air, the performance of the Bio-Air and the CathRec configurations were compared. For the CathRec, the SOFC-DIS operates at split fraction of 0.5 which means that half of the cathode outlet stream is recycled and mixed with fresh air while the rest of cathode stream is fed to the afterburner. It

Table 5
System performance and total cost index of the SOFC-DIS with different configurations.

	Overall electrical efficiency (%)	CHP efficiency (%)	Total cost index
No-HX (base case)	15.79	76.45	1.000
CondBio	16.26	78.73	0.965
HW-Bio	16.21	78.48	0.969
Cond-Air	16.95	81.74	0.948
CathRec	21.67	79.87	0.662
CondBio-CathRec	22.53	74.71	0.641

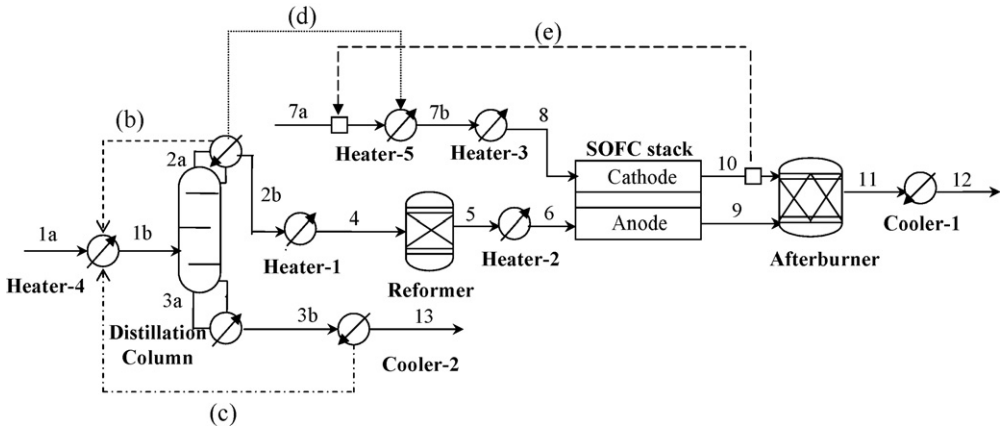

Fig. 5. Schematic diagram of SOFC-DIS systems: (a) No-HX, (b) CondBio, (c) HW-Bio, (d) Cond-Air and (e) CathRec at the base conditions (C_{EtOH} = 25%, EtOH recovery = 80%, U_f = 80%, V = 0.7 V, T_{SOFC} = 1200 K, $T_{anode,in}$ = 1100 K, $T_{cath,in}$ = 1000 K, T_{RF} = 1023 K and P = 101.3 kPa).

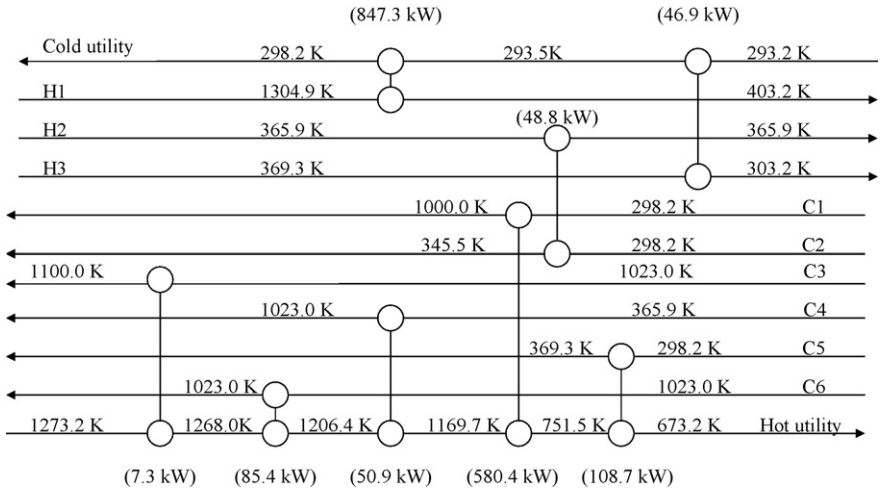

Fig. 6. Heat exchanger network of SOFC-DIS (CondBio) at the base conditions (C_{EtOH} = 25%, EtOH recovery = 80%, U_f = 80%, V = 0.7 V, T_{SOFC} = 1200 K, $T_{anode,in}$ = 1100 K, $T_{cath,in}$ = 1000 K, T_{RF} = 1023 K and P = 101.3 kPa).

should be noted that the heat recovery from hot water to preheat incoming air has not been studied because the heat cannot be fully transferred as mentioned earlier in the previous section. From the results, Table 5, the CHP efficiency for both the Bio-Air configuration and the CathRec configuration shows similar potential. However, the overall electrical efficiency of the CathRec configuration is 5% higher than that of the Bio-Air. In addition, the total cost index of the CathRec configuration is 28% lower than that of the Bio-Air config-

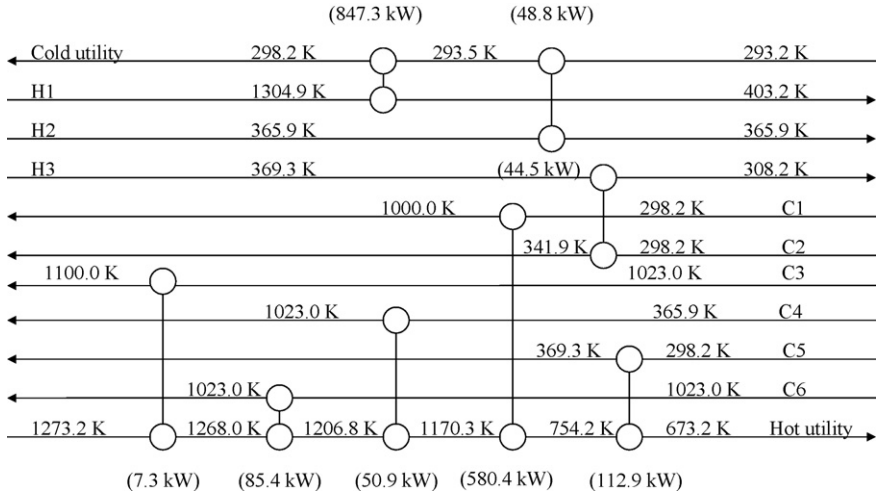

Fig. 7. Heat exchanger network of SOFC-DIS (HW-Bio) at the base conditions (C_{EtOH} = 25%, EtOH recovery = 80%, U_f = 80%, V = 0.7 V, T_{SOFC} = 1200 K, $T_{anode,in}$ = 1100 K, $T_{cath,in}$ = 1000 K, T_{RF} = 1023 K and P = 101.3 kPa).

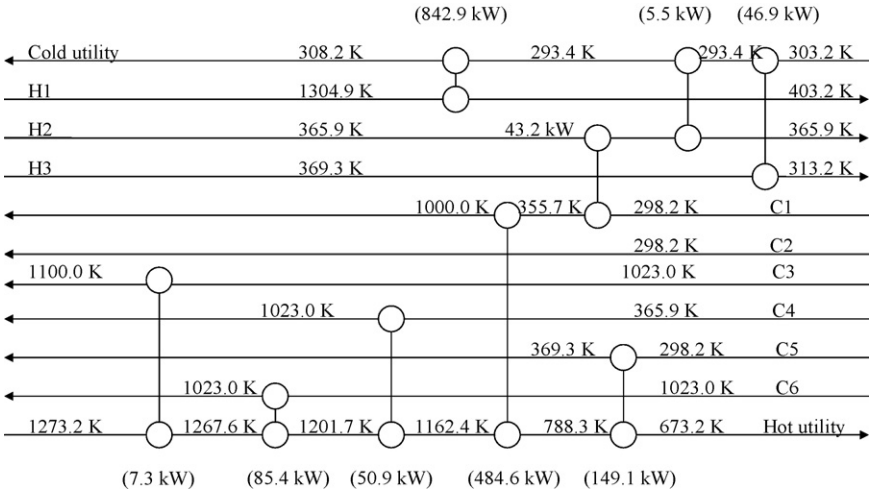

Fig. 8. Heat exchanger network of SOFC-DIS (Cond-Air) at the base conditions (C_{EtOH} = 25%, EtOH recovery = 80%, U_f = 80%, V = 0.7 V, T_{SOFC} = 1200 K, $T_{anode,in}$ = 1100 K, $T_{cath,in}$ = 1000 K, T_{RF} = 1023 K and P = 101.3 kPa).

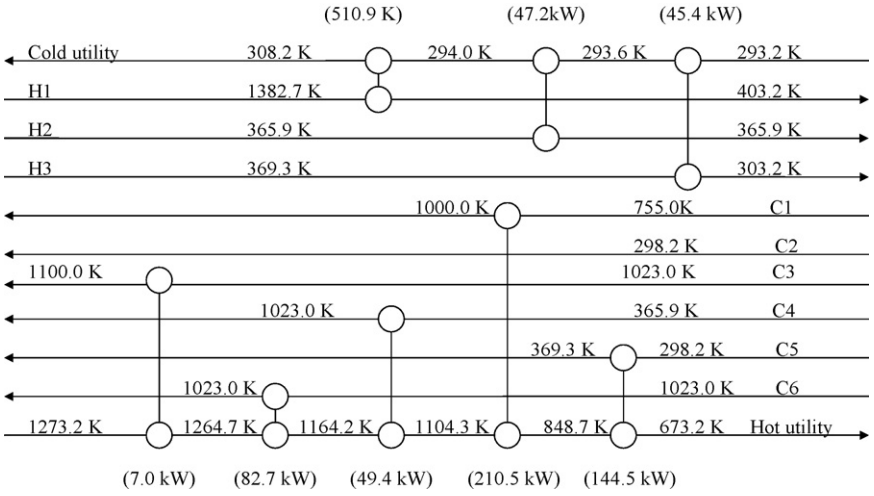

Fig. 9. Heat exchanger network of SOFC-DIS (CathRec) at the base conditions with Sp = 0.5 (C_{EtOH} = 25%, EtOH recovery = 80%, U_f = 80%, V = 0.7 V, T_{SOFC} = 1200 K, $T_{anode,in}$ = 1100 K, $T_{cath,in}$ = 1000 K, T_{RF} = 1023 K and P = 101.3 kPa).

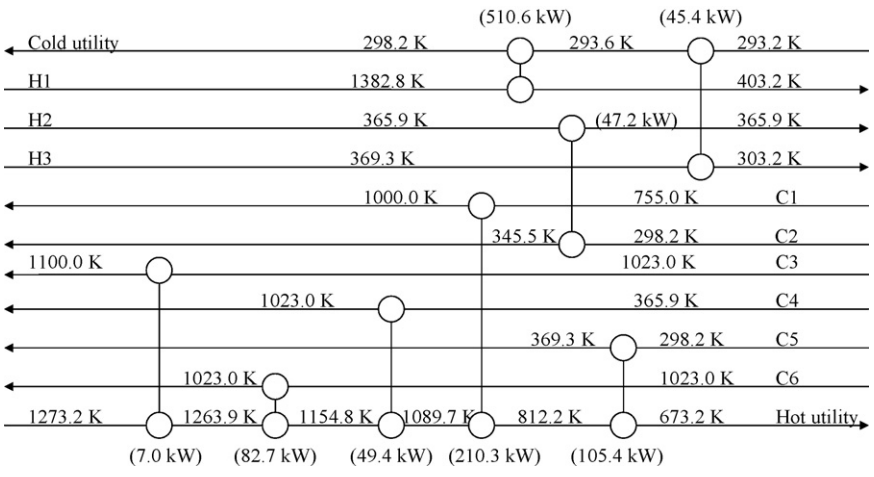

Fig. 10. Heat exchanger network of SOFC-DIS (CondBio-CathRec) at the base conditions with Sp = 0.5 (C_{EtOH} = 25%, EtOH recovery = 80%, U_f = 80%, V = 0.7 V, T_{SOFC} = 1200 K, $T_{anode,in}$ = 1100 K, $T_{cath,in}$ = 1000 K, T_{RF} = 1023 K and P = 101.3 kPa).

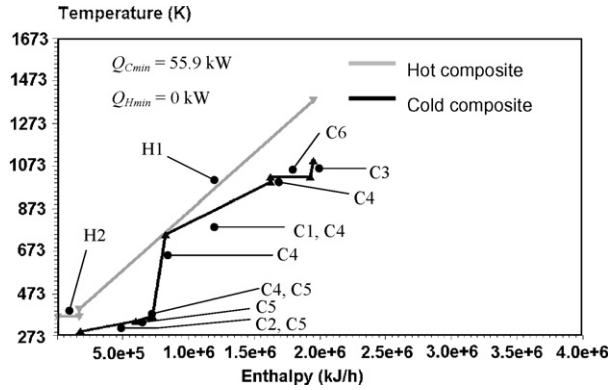

Fig. 11. Composite curves of SOFC-DIS (CondBio-CathRec) at base conditions with $Sp = 0.5$ (C_{EtOH} = 25%, EtOH recovery = 80%, U_f = 80%, V = 0.7 V, T_{SOFC} = 1200 K, $T_{anode,in}$ = 1100 K, $T_{cath,in}$ = 1000 K, T_{RF} = 1023 K and P = 101.3 kPa).

uration, therefore, the CathRec configuration is selected to preheat the incoming SOFC air. The Bio-Cond and the CathRec configurations are then combined, so-called CondBio-CathRec, and chosen to be further designed for a process-to-process heat exchanger network. It can be noticed that the CondBio-CathRec configuration yields the highest overall electrical efficiency and the lowest total cost index as shown in Table 5. The heat exchanger network for the CondBio-CathRec configuration is also presented in Fig. 10. The amount of utility for Q_C = 566.0 kW and Q_H = 454.8 kW are required. Noticeably, high amount of hot and cold utility are still needed. The composite curve of the CondBio-CathRec configuration at the base conditions with $Sp = 0.5$ when ΔT_{Min} is set at 10 K is presented in Fig. 11. The narrowest gap in the threshold problem is so called 'pseudo-pinch' and in this case, it is located at the air inlet temperature. The base conditions with $Sp = 0.5$ is still a threshold problem with Q_{Cmin} = 55.9 and Q_{Hmin} are 0 kW, respectively. Clearly, the heat exchanger network for the CondBio-CathRec in Fig. 10 needs more work to be done to reach an MER network.

The design of the threshold case follows the same rules as that of the pinch case. To design a MER network, it is necessary to design the heat exchanger network above and below the pseudo-pinch point separately because the pseudo-pinch is in the middle of the composite curves. The following rules for the MER design are required [14].

(1) No cold utility is used above the pinch point.
(2) No hot utility is used below the pinch point.
(3) No heat transfer across the pinch point.

The heat capacity (MC_p) of each stream at the base conditions with $Sp = 0.5$ are presented in Table 6. Overall, there are two hot streams (a hot flue gas from the afterburner (H1) and heat recovery from the condenser (H2)) and six cold streams (e.g. a syngas stream (C3), a reformer (C6), a distillate stream (C4), an air stream (C1), a reboiler (C5) and a bioethanol inlet (C2)). However, it should be noted that the heat recovery from the condenser has to be matched with the bioethanol inlet as the CondBio is selected for preheating the incoming bioethanol. For the design above pseudo-pinch, the MC_p of the hot stream has to be lower than the cold stream near the pseudo-pinch point in order to avoid the temperature crossover [14]. The possible cold streams that can be matched with the hot stream near the pinch point are the reformer and the air stream. However, when the reformer is the last unit which is near the pseudo-pinch point, the hot flue gas cannot supply heat to the reformer due to low inlet temperature for heat exchange. Consequently, the hot flue gas cannot be cooled down to the pseudo-pinch temperature using process streams. Cold utility is required above the pseudo-pinch and this violates the rule for MER design. Therefore, the only configuration which ends with the air heat exchanger is considered for the above pseudo-pinch design. Below the pseudo-pinch, one hot stream and two cold streams (e.g. a distillate stream (C4) and a reboiler (C5) are considered. It is known that the MC_p of the hot stream must be higher than that of the cold stream near the low-temperature pinch point [14]. From Table 6, only the MC_p of the distillate is higher than that of the hot flue gas. Therefore, only one match is possible. The hot stream has to exchange heat with the distillate and then with the reboiler. From these preliminary considerations, there are six possible MER designs, D1 through D6, for the pinch case. The sequences of heat exchanging for MER designs are listed as follows. The first stream label is the first cold stream to be heat exchanged with hot stream and so on.

- D1: C3–C4–C6–C1–C4–C5
- D2: C3–C6–C4–C1–C4–C5
- D3: C4–C3–C6–C1–C4–C5
- D4: C4–C6–C3–C1–C4–C5
- D5: C6–C3–C4–C1–C4–C5
- D6: C6–C4–C3–C1–C4–C5

The total cost index of all six designs is presented in Table 7. All six MER designs have the target energy of 21.2 and 62.5 kW for hot utility and cold utility, respectively. From the results, it can be seen that the total cost index for all six designs are similar but Design D2, C3–C6–C4–C1–C4–C5 shows the lowest total cost index from the six considered among other designs and is then chosen for a further design. The heat exchanger network of D2 MER design is next presented in Fig. 12. The utility meets the utility targets at Q_{Cmin} = 55.9 and Q_{Hmin} = 0. Obviously, changing process structure by implementing cathode recirculation and adding one more heat exchanger to preheat incoming bioethanol can reduce Q_{Cmin} from 73.4 kW (for the No-HX case) to 55.9 kW. It should be noted that although all six MER configurations (D1–D6) are somewhat complex from operability point of view and one should the tradeoff between annualised cost and complexity; one maybe able to simplify the design how-

Table 6
Information of each unit operated at the base condition (threshold problem).

Stream no.	Stream label	T_{in} (K)	T_{out} (K)	Load (kW)	MC_p (kW K^{-1})
Hot stream					
Cooler-1 (11–12)	H1	1382.9	403.0	510.6	0.521
Condenser (2a–2b)	H2	366.0	366.0	47.2	Large
Cold stream					
Air stream (7b–8)	C1	755.0	1000.0	210.3	0.858
BioEtOH stream (1a–1b)	C2	298.2	345.7	47.2	0.994
Syngas stream (5–6)	C3	1023.0	1100.0	7.0	0.091
Distillate stream (2–4)	C4	366.0	1023.0	49.4	0.075
Reboiler (3a–3b)	C5	298.2	369.3	105.4	1.482
Reformer (4–5)	C6	1023.0	1023.0	82.7	Large

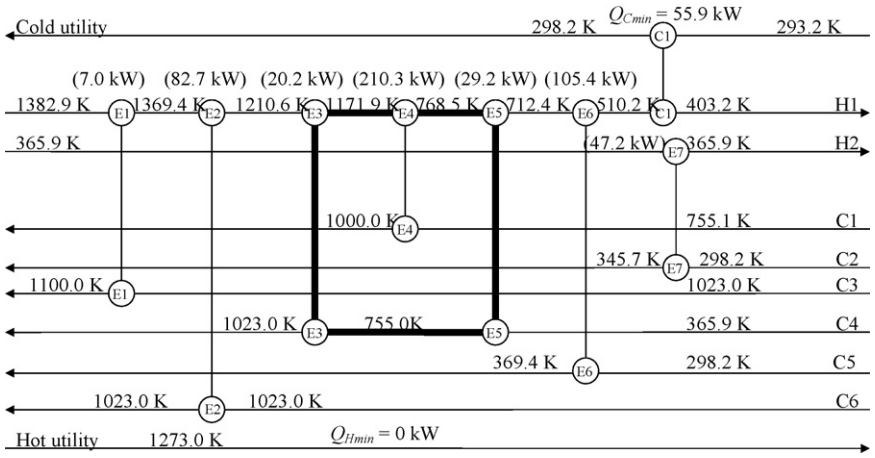

Fig. 12. The MER design of SOFC-DIS (CondBio-CathRec) at the base conditions with $Sp = 0.5$ (C_{EtOH} = 25%, EtOH recovery = 80%, U_f = 80%, V = 0.7 V, T_{SOFC} = 1200 K, $T_{anode,in}$ = 1100 K, T_{RF} = 1023 K and P = 101.3 kPa).

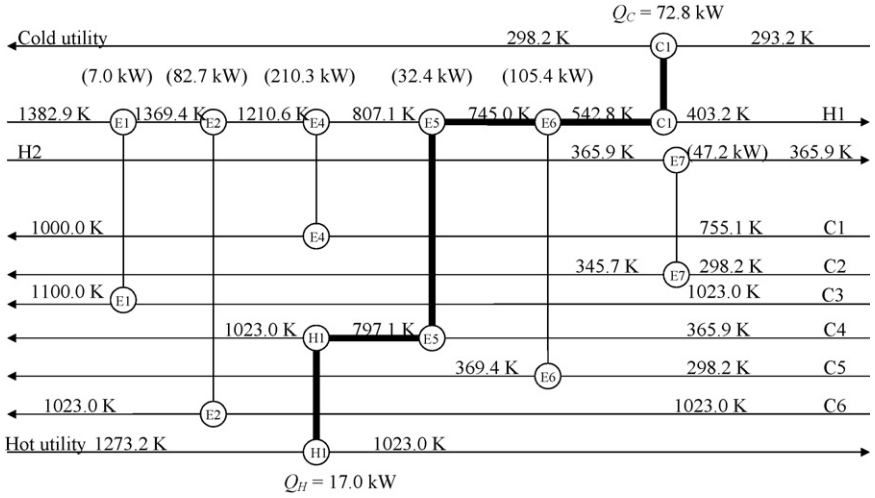

Fig. 13. The design of SOFC-DIS (CondBio-CathRec) without E3 at the base conditions with $Sp = 0.5$ (C_{EtOH} = 25%, EtOH recovery = 80%, U_f = 80%, V = 0.7 V, T_{SOFC} = 1200 K, $T_{anode,in}$ = 1100 K, T_{RF} = 1023 K and P = 101.3 kPa).

ever it will no longer be an MER design and will cost more. Clearly, the distillate stream requires two heat exchangers for heating up to the target temperature, one high temperature heat exchanger (E3) and one low-temperature heat exchanger (E5) and results in an E3–E5–E5–E3 loop in all configurations as shown by the dark line in Fig. 12. Two heat exchanges are present on the distillate stream and this loop results in the complexity of the design and operability difficulties. In an attempt to simplify the network we removed one of the heat exchangers on the distillate stream; however, it is not obvious which ones of the distillate heat exchangers should be eliminated. Table 8 shows the operating cost index, capital cost index and total cost index for different cases. In this section, the total cost index can be calculated by the ratio of total cost of each design to the total cost of the MER design at the base conditions with $Sp = 0.5$. The total costs index follow the sequence of C3–C6–C1–C4–C5 (base-no E3 case) ≈ C3–C6–C4–C1–C5 (base-no E5 case) < MER case. The operating cost index of the base-no E3 case is lower than that of the base-no E5 case because large amount of heating utility

Table 7
Total cost index for different designs.

Configuration	Total cost index[a]
No-HX CondBio-CathRec (base case)	1.000
D1 (C3–C4–C6–C1–C4–C5)	0.3559
D2 (C3–C6–C4–C1–C4–C5)	**0.3556**
D3 (C4–C3–C6–C1–C4–C5)	0.3559
D4 (C4–C6–C3–C1–C4–C5)	0.3565
D5 (C6–C3–C4–C1–C4–C5)	0.3559
D6 (C6–C4–C3–C1–C4–C5)	0.3562

[a] Operate at the base condition (C_{EtOH} = 25%, EtOH recovery = 80%, U_f = 80%, V = 0.7 V, T_{SOFC} = 1200 K, $T_{anode,in}$ = 1100 K, T_{RF} = 1023 K and P = 101.3 kPa).

Table 8
Cost estimation of the SOFC-DIS of different scenarios.

	Operating cost index	Capital cost index	Total cost index
Threshold problem			
Base condition-MER	1.000	1.000	1.000
Base-no E3	7.381	0.930	0.996
Base-no E5	11.31	1.018	1.124
Base-no E3-no path	19.55	0.826	1.020
Avoiding pinch (based on MER design)			
1173 K	8.719	1.102	1.181
1173 K–Uf75	2.093	0.848	0.860
1173 K–Sp0.3	0.442	1.077	1.071
1173 K–Sp0.7	1.407	0.836	0.841

is required to heat up air stream to meet the target temperature for the case of base-no E5. However, the base-no E3 case requires two heaters to heat up both distillate stream and air stream and results in higher capital cost index but still lower than that of the MER case.

The benefit of eliminating path of utility is also investigated. As shown in Fig. 13, there is a path connecting the cold and hot utilities via the distillate heater shown by the dark line. The total cost index of the case of no path (base-no E3-no path) and the base-no E3 are compared and presented in Table 8. It was found that the total cost index of the case without path way is higher than that of the base-no E3. This is because the operating cost of the base-no E3-no path is almost three times higher than that of with path. Therefore, it can be concluded that the base-no E3 is the most preferable. One heater has to be located after the distillate heat exchanger. The corresponding performances of this design are 40.8%, 54.3%, 0.221 W cm^{-2} for overall electrical efficiency, CHP efficiency and power density, respectively.

3.2.2. Effect of operating conditions

The effect of operating conditions (e.g. ethanol recovery, ethanol concentration, fuel utilization, voltage, split fraction, SOFC temperature, cathode inlet temperature) on the composite curves was first investigated. The EtOH recovery and C_{EtOH} are in the range

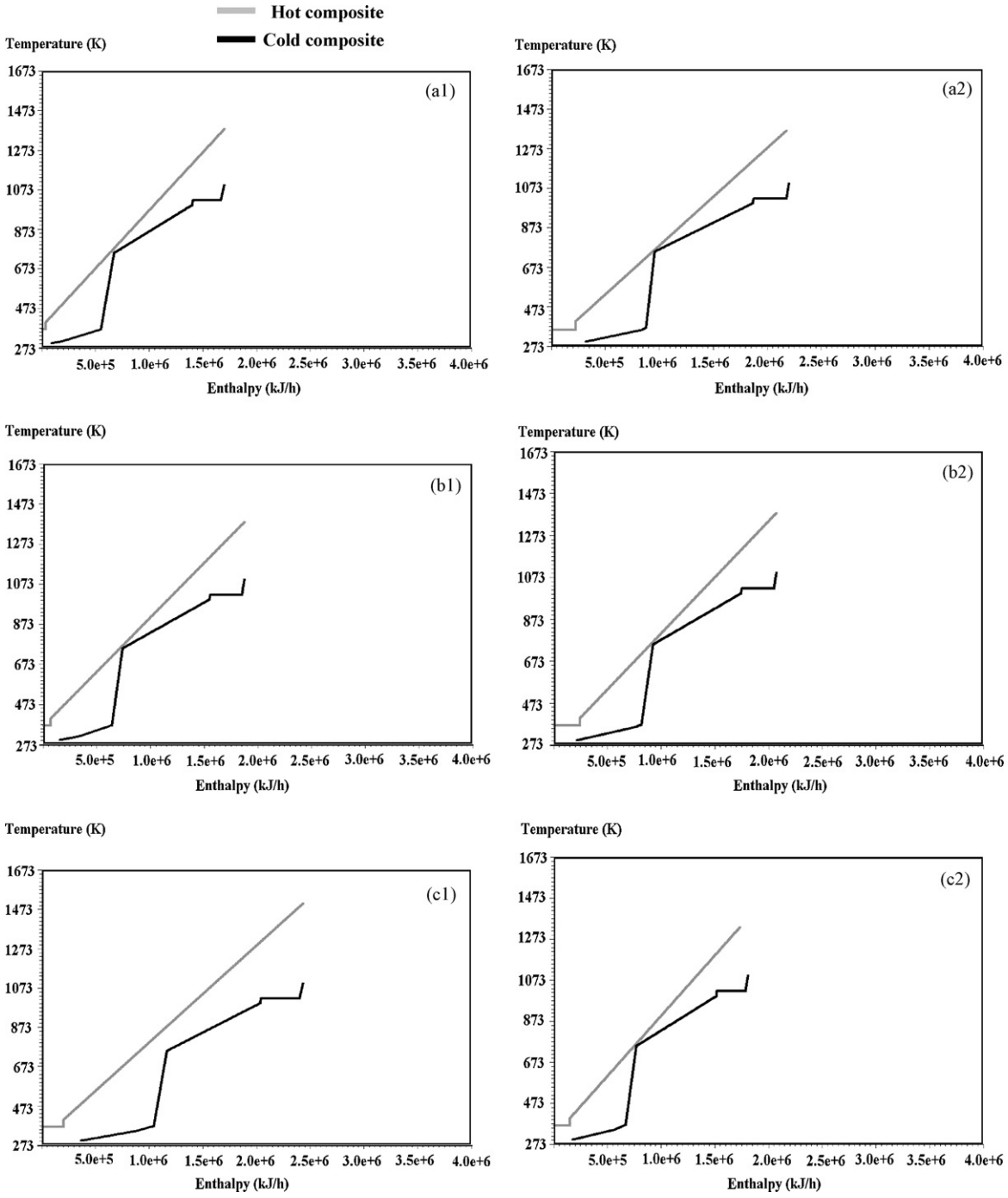

Fig. 14. Composite curves of SOFC-DIS at different operating conditions: (a1) C_{EtOH}, = 17 mol%, (a2) C_{EtOH}, = 41 mol%, (b1) EtOH recovery = 70%, (b2) EtOH recovery = 90%, (c1) V = 0.65 V, (c2) V = 0.75 V, (d1) U_f = 75%, (d2) U_f = 85%, (e1) Sp = 0.3, (e2) Sp = 0.7, (f) T_{SOFC} = 1173 K, (g) $T_{cath,in}$ = 1100 K.

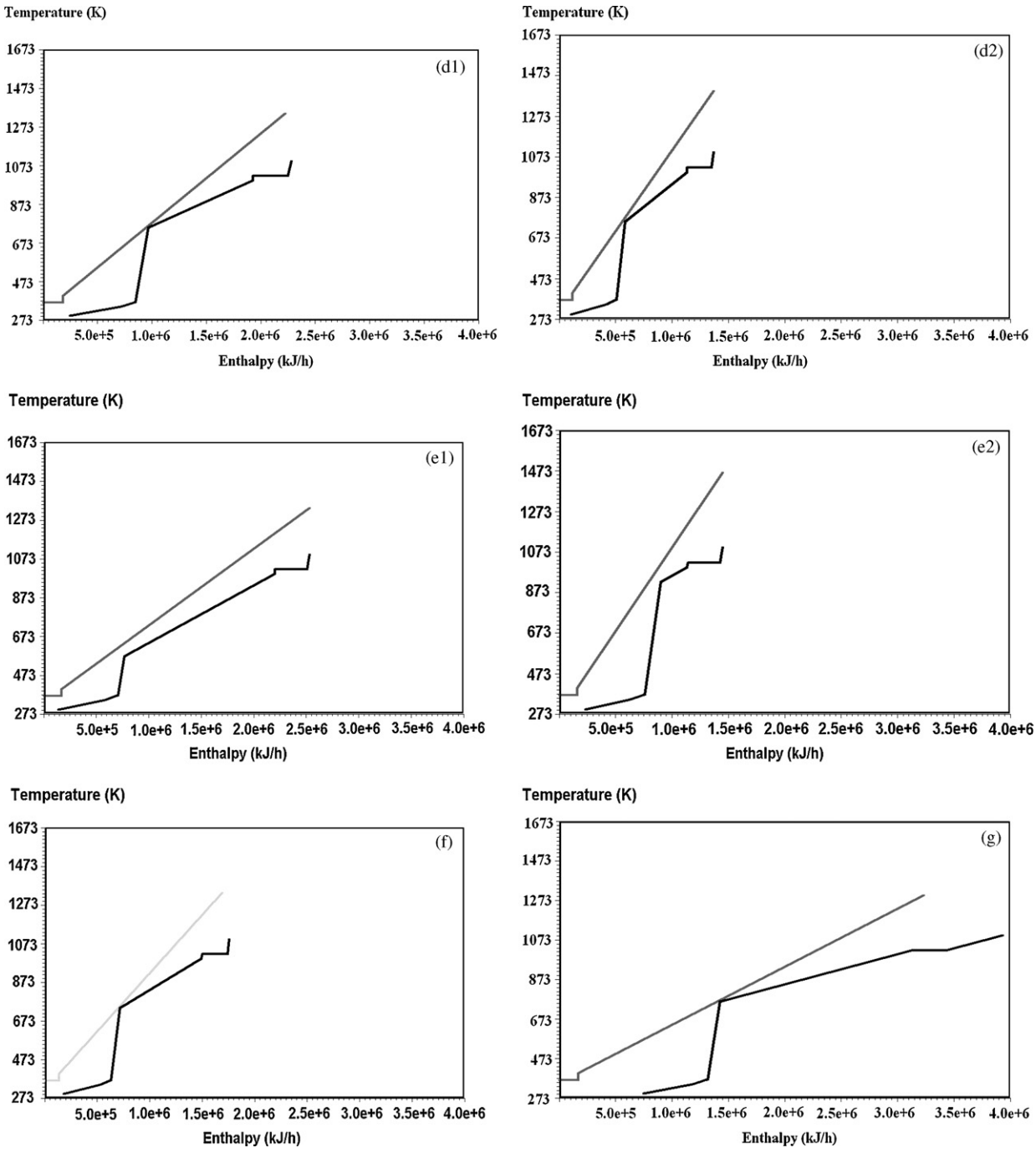

Fig. 14. (*Continued*).

of 70–90% and 17–41 mol%, respectively. It should be noted that the maximum ethanol concentration that can be fed to the external reformer without carbon formation is 41 mol% [9]. Also, in this study, only high ethanol recovery is considered due to high SOFC efficiency. Fuel utilization and voltage were varied from 70 to 85% and 0.65 to 0.75 V, respectively and the split fraction was varied from 0.3 to 0.7. The SOFC temperature of 1173 K and the cathode inlet temperature of 1100 K were examined. Fig. 14 shows the composite curves at these different conditions. Noticeably, it can be seen that the distillation parameters (e.g. ethanol concentration and recovery) does not have significant effect on the composite curves. For SOFC operating conditions, voltage, fuel utilization and split fraction have a strong effect on the composite curves. For the effect of voltage, the higher the voltage, the steeper the composite curves. This can be explained that the lower voltage relates to higher amount of heat loss within the SOFC stack. Therefore, to maintain the temperature inside the stack, more air is required, resulting in lower outlet temperature from the afterburner and higher heat capacity of hot stream. It should be noted that the slope of composite curve is inverse with heat capacity of the streams. Hence, the less steep slope of the hot composite curve is obtained. Moreover, because more air is required for cooling the stack, more heat is needed at the air heater and results in less steep slope of the cold composite curve as illustrated in Fig. 14(c1). In addition, for a lower U_f, more unreacted fuel is burnt in the afterburner and this results in a higher outlet temperature of the hot flue gas and

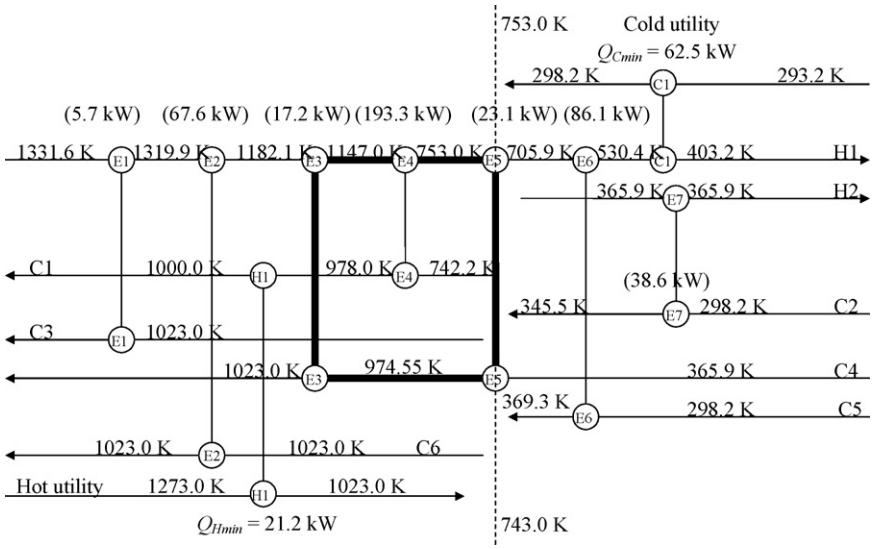

Fig. 15. MER design of SOFC-DIS (CondBio-CathRec) (C_{EtOH} = 25 mol%, EtOH recovery = 80%, U_f = 80%, V = 0.7 V, Sp = 0.5, T_{SOFC} = 1173 K, $T_{anode,in}$ = 1100 K, $T_{cath,in}$ = 1000 K, T_{RF} = 1023 K and P = 101.3 kPa).

more heat recovered from the afterburner as shown in Fig. 14(d1). Consequently, the cold composite curve moves horizontally toward the hot composite curve until it reaches the threshold case in which no hot utility is required. For the higher U_f (in this case, U_f = 85%), the lower temperature of the hot flue gas is obtained. The cold composite curve moves horizontally to the hot composite curve and reaches the pinch point before it meets the threshold condition.

The effect of split fraction was investigated. At low split fractions, a lower amount of high temperature air from the cathode is mixed with the fresh air; therefore, lower air inlet temperature and more energy is consumed in the air heater. Consequently, the slope of the cold stream, especially that of the air heater, decreases and the location of the kink on the cold stream changes. Noticeably, the outlet temperature of hot flue gas from the afterburner is lower because more air, heat carrier, is burnt inside the afterburner. The less steep hot stream can be detected due to higher amount of air in the hot flue gas stream. Higher split fractions result in a larger amount of air to be mixed with the fresh air. A higher air inlet temperature and the lower energy consumption at the air heater were observed. However, when the amount of air fed to the afterburner is reduced, the outlet temperature of the hot stream is higher. Also, lower amount of air in the hot flue gas results in a steeper slope of the hot stream.

From the results, the composite curves can be divided into two groups: (1) the pinch problem and (2) the threshold problem. For the pinch case, the conditions that were found to cause a pinch point in the composite curves are: C_{EtOH} of 41 mol%, operating voltage of 0.65 V, cathode inlet temperature of 1100 K, SOFC temperature of 1173 K and U_f of 85%. Other conditions resulted in the threshold case. The MER design for the pinch case when T_{SOFC} = 1173 K are presented in Fig. 15. The heat capacity and heat load for each stream are presented in Table 9. It can be noticed that Q_{Cmin} = 62.5 and Q_{Hmin} = 21.2 kW. The total cost index is compared to that of the threshold case at the base conditions with Sp = 0.5 in Table 8. It should be noted that the total cost indexes for the pinch case are calculated based on the total cost of the base-MER cases; therefore, the total cost index of the pinch case can be directly compared to that of the threshold cases. Table 8 shows that operating at T_{SOFC} = 1173 K yields higher operating cost, capital cost and total cost than the base-no E3 case.

3.2.3. Avoiding a pinch point by operating at different conditions

As mentioned earlier, the pinch point was found when operating at C_{EtOH} = 41 mol%, T_{SOFC} = 1173 K, $T_{cath,in}$ = 1100 K, U_f = 85% or V = 0.65 V. It can be noticed that the pinch point occurs at the air inlet temperature; therefore, we investigated the effect of the SOFC-DIS operating conditions on the pinch point. As shown in Fig. 14, the shape of composite curves changes dramatically when U_f, split fraction or voltage change. In this case, only split fraction and fuel utilization are considered. It should be noted that adjusting voltage is not considered in this study because it directly affects the SOFC stack performance. In addition, lower split fraction, higher split fraction and lower fuel

Table 9
Information of each unit operated under pinch problem.

Stream no.	Stream label	T_{in} (K)	T_{out} (K)	Load (kW)	MC_p (kW K^{-1})
Hot stream					
Cooler-1 (11–12)	H1	1331.6	403.0	455.5	0.486
Condenser (2a–ab)	H2	365.9	365.9	38.6	Large
Cold stream					
Air stream (7b–8)	C1	742.1	1000.0	214.5	0.832
BioEtOH stream (1a–1b)	C2	298.2	345.5	48.4	1.023
Syngas stream (5–6)	C3	1023.0	1100.0	5.7	0.074
Distillate stream (2–4)	C4	365.9	1023.0	40.3	0.061
Reboiler (3a–3b)	C5	298.2	369.4	86.1	1.209
Reformer (4–5)	C6	1023.0	1023.0	67.6	Large

utilization are examined. As mentioned in the preceding section, lower split fraction reduces the slope of the cold stream and the kink at the air heater occurs at a lower temperature; this could eliminate the pinch point. For higher split fractions, steeper hot composite curves could also help avoiding the pinch point as shown in the wider gap between the hot and cold composite curves in Fig. 14(e). Lastly, operating at lower fuel utilization can make the hot composite curve have higher outlet temperature and probably affect the gap between the composite curves.

For T_{SOFC} = 1173 K, the results show that when the SOFC-DIS operates at a higher split ratio (Sp = 0.7) or lower value (Sp = 0.3) or lower U_f = 75%, the pinch point disappears and a threshold problem is obtained. At U_f = 85%, operating SOFC-DIS at Sp = 0.7 or 0.3 the pinch point disappears. The total cost index of the pinch case and the threshold case are compared and shown in Table 8. When the SOFC-DIS operates at threshold conditions, lower total cost index is obtained for all cases. The total cost index are in the sequence of 1173 K–Sp = 0.7 < 1173 K–U_f = 75% < 1173 K–Sp = 0.3. In addition, it can be seen that the 1173 K–Sp = 0.7 and 1173 K–U_f = 75% yield lower total cost index than that of base-no E3 case. This can be implied that adjusting operating conditions can lower the total cost index at the base conditions.

4. Conclusions

The performance of a thermally integrated SOFC system integrated with a distillation column (SOFC-DIS) was presented in this study. The heat exchanger network of the SOFC-DIS without thermal integration (No-HX SOFC-DIS) at the base conditions was first investigated. Q_{Cmin} of 73.4 kW and Q_{Hmin} of 0 kW were required. The improvement of SOFC-DIS by changing process structure and utilizing internal heat sources (e.g. condenser duty and hot water from the bottom of the distillation column) was then examined. It was found that a utilization of condenser duty to preheat an incoming bioethanol and a cathode recirculation significantly helped reducing an energy demand for the reboiler and the air heater, respectively and resulted in higher overall electrical efficiency and lower total cost index. The system configuration is so-called 'CondBio-CathRec'. The MER network for the CondBio-CathRec was then obtained. It was found that the MER network can reduce Q_{Cmin} of 73.4 kW in No-HX case to 55.9 kW. The heat exchanger loop and utility path in MER network were further studied. It was found that eliminating high temperature distillate heat exchanger (E3) yields the lowest total cost index. Conclusively, the recommended network for SOFC-DIS at the base condition is C3–C6–C1–C4–C5 that means the hot effluent from the afterburner was designed to provide heat to an anode heat exchanger first and then an external reformer, an air heat exchanger, a distillate downstream heat exchanger and finally a reboiler. The effect of operating conditions on the network was then investigated. The results were found that no pinch point occurs except for C_{EtOH} = 41 mol% or the cathode inlet temperature of 1100 K or T_{SOFC} = 1173 K or U_f = 85%. The MER network for the pinch case when T_{SOFC} = 1173 K was investigated and found the higher total cost index. Lastly, the results showed that T_{SOFC} = 1173 K can become a threshold case when operating at lower/higher split fraction or lower fuel utilization. The results found that the obtained threshold problem yields lower total cost indexes than that of the pinch case (T_{SOFC} = 1173 K). Moreover, it can be noticed that changing operating conditions (e.g. lower fuel utilization or higher split fraction) can achieve the lower total cost index than that of the base conditions. Suitable operating conditions which yield the lowest total cost index should be further investigated.

Acknowledgements

The support from the Thailand Research Fund, Commission of High Education and National Metal and Materials Technology Center (MTEC) are gratefully acknowledged.

References

[1] E. Fontell, T. Kivisaari, N. Christiansen, J.B. Hansen, J. Pålsson, J. Power Sources 131 (2004) 49–56.
[2] A.O. Omosun, A. Bauen, N.P. Brandon, C.S. Adjiman, D. Hart, J. Power Sources 131 (2004) 96–106.
[3] W. Zhang, E. Croiset, P.L. Douglas, M.W. Fowler, E. Entchev, Energy Convers. Manage. 46 (2005) 181–196.
[4] R.J. Braun, S.A. Klein, D.T. Reindl, J. Power Sources 158 (2006) 1290–1305.
[5] S. Douvartzides, F.A. Coutelieris, P.E. Tsiakaras, J. Power Sources 114 (2003) 203–212.
[6] S. Douvartzides, F. Coutelieris, P. Tsiakaras, J. Power Sources 131 (2004) 224–230.
[7] L.E. Arteaga, L.M. Peralta, V. Kafarov, Y. Casas, E. Gonzales, Chem. Eng. J. 136 (2008) 256–266.
[8] W. Jamsak, S. Assabumrungrat, P.L. Douglas, N. Laosiripojana, R. Suwanwarangkul, S. Charojrochkul, ECS Trans. 7 (2007) 1475–1482.
[9] S. Assabumrungrat, V. Pavarajarn, S. Charojrochkul, N. Laosiripojana, Chem. Eng. Sci. 59 (2004) 6015–6020.
[10] E.Y. Garcia, M.A. Laborde, Int. J. Hydrogen Energy 16 (1991) 307–312.
[11] K. Vasudeva, N. Mitra, P. Umasankar, S.C. Dhinggra, Int. J. Hydrogen Energy 21 (1996) 13–18.
[12] E. Achenbach, J. Power Sources 49 (1994) 333–348.
[13] S.H. Chan, C.F. Low, O.L. Ding, J. Power Sources 103 (2002) 188–200.
[14] B. Linnhoff, D.W. Townsend, D. Boland, G.F. Hewitt, B.E.A. Thomas, A.R. Guy, R.H. Marsland, User Guide on Process Integration for the Efficient Use of Energy, 1st edition, Institution of Chemical Engineering, UK, 1982.